ELSEVIER

Ceramics International 27 (2001) 149–155

CERAMICS INTERNATIONAL

Electrochemical deposition of ceria and doped ceria films

I. Zhitomirsky *, A. Petric

Department of Materials Science and Engineering, McMaster University, 1280 Main Street West, Hamilton, ON, Canada L8S 4L7

Received 19 April 2000; received in revised form 3 May 2000; accepted 9 May 2000

Abstract

Cathodic electrodeposition of CeO_2 and $Ce_{1-x}Gd_xO_{2-y}$ was performed from aqueous and mixed ethyl alcohol-water solutions of $CeCl_3$ and $GdCl_3$ on Ni foil and Ni–yttria stabilized zirconia substrates. The influence of hydrogen peroxide on the electrodeposition process was studied. Electrochemical intercalation of poly(diallyldimethylammonium chloride) into the deposits was demonstrated and the mechanism of intercalation is discussed. The experimental results indicate that the polymer acts as a binder, providing better adhesion of the organoceramic deposits and reducing cracking while allowing for film formation on porous substrates. The deposits were studied by X-ray diffraction, thermogravimetric analysis and scanning electron microscopy.

Keywords: A. Films; A. Tape casting; B. Composites; D. CeO_2

1. Introduction

A number of reports have showed that CeO_2 films are effective for corrosion inhibition in aqueous environments and protection of metals and alloys from high temperature corrosion [1,2]. There is a growing interest in electronic applications of ceria films [3]. CeO_2 and doped ceria films are of considerable interest for applications in solid oxide fuel cells operating at reduced temperatures [4–7]. In addition to their proposed use in anodes and electrolytes, ceria thin films could serve to prevent interfacial electrolyte–electrode degradation and corrosion of interconnects. Thin layers of doped ceria on the YSZ electrolytes yielded reduced interfacial resistance at cathodes and anodes and as a result higher power densities of fuel cells were achieved [5,7].

Applications of ceria films are invariably linked to advances in deposition techniques. Cathodic electrolytic deposition is evolving as an important method in ceramic processing [8–13]. The interest in this technique stems from a variety of reasons such as low cost of equipment, rigid control of deposit thickness and uniformity as well as the possibility of forming coatings on substrates of complex shape [8,14]. Cathodic deposition of ceria has been reported in several papers [15–21]. Although both $CeCl_3$ and $Ce(NO_3)_3$ solutions have been used, the more adherent and uniform coatings were obtained from chloride baths [20]. Atomic force microscopy studies [21] indicate that electrodeposition of ceria occurs through a nucleation and growth mechanism.

Rare-earth doped cerium oxides exhibit high oxygen ionic conductivity, which makes them important materials for applications in solid oxide fuel cells. Recently, we reported [22] that gadolinium oxide films could be deposited using cathodic electrolytic deposition. These results pave the way for electrodeposition of ceria films doped with gadolinium oxide. An important advance was the discovery of electrochemical intercalation of a cationic polyelectrolyte into electrolytic gadolinium hydroxide deposits [22]. It was demonstrated that by using poly(dimethyldiallylammonium chloride) (PDDA) as a cationic polyelectrolyte with inherent binding properties, problems related to cracking in electrolytic deposits could be diminished. Moreover we have demonstrated the formation of nanostructured organoceramic materials via cathodic electrodeposition.

This paper presents the results of electrolytic deposition of ceria and doped ceria films, and discusses the mechanism of deposition and influence of additives on deposit morphology and crystallization behavior.

* Corresponding author. Fax: +1-905-528-9295.
E-mail address: zhitom@mcmaster.ca (I. Zhitomirsky).

0272-8842/01/$20.00
PII: S0272-8842(00)00054-7

2. Experimental procedures

2.1. Electrodeposition

Commercial purity $CeCl_3$, $GdCl_3 \cdot 6H_2O$ (Alfa Aesar), H_2O_2 (30 wt.% in water, BDH Inc.), and poly(-diallyldimethylammonium chloride) (Aldrich) were used as starting materials. A schematic of the structure of PDDA is shown in Fig. 1. Aqueous and ethanol–water (10 vol.% water) solutions of $CeCl_3$ and $(1-x)$ $CeCl_3 + x$ $GdCl_3$ ($x = 0$–0.3) were prepared. Cathodic electrolytic deposition experiments were performed from the solutions saturated with air or solutions containing 0.025 M H_2O_2 additive. Cerium salt concentration was in the range 0.5–10 mM.

Electrodeposition experiments were performed in the galvanostatic mode at current densities ranging from 1 to 5 mA/cm^2. Cathodic deposits were obtained on Ni (60× 60×0.1 mm) and Ni–YSZ cermet substrates prepared using tape casting technology. Before deposition, the substrates were washed with deionized water, rinsed with ethanol in an ultrasonic bath and dried in air. Deposition times of up to 20 min. were used. The electrochemical cell included the cathodic substrate centered between two co-planar platinum counter electrodes. The deposits obtained were washed with water and dried in air. After drying at room temperature, the electrolytic deposits were scraped from the Ni electrodes for X-ray diffraction and thermal analysis. Deposit weights were determined by difference in electrode weight before and after deposition followed by drying at room temperature for 72 h.

2.2. Preparation of cermet substrates

Porous Ni–YSZ substrates were prepared by tape casting. Nickel oxide (Inco, F-grade) and yttria stabilized zirconia YSZ (TZ-8Y, Tosoh) comprised the ceramic powders in the formulation of the slurry (Table 1). A mixture of toluene and ethyl alcohol was used as a solvent. Z-3 Blown Menhadeh fish oil, polyvinyl butyral

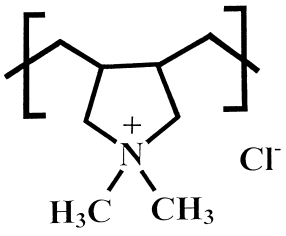

PDDA

Fig. 1. Schematic structure representation of PDDA.

Table 1
Slurry composition for tape casting of Ni–YSZ cermet

Material	Function	wt.%
NiO	Powder	38.1
YSZ	Powder	25.4
Ethyl alcohol	Solvent	10.8
Toluene	Solvent	16.1
Fish oil	Dispersant	1.1
PVB	Binder	3.1
Butyl benzyl phthalate	Plasticizer	5.4

(Butvar, B79) and butyl benzyl phthalate (S-160) were chosen as dispersant, binder and plasticizer, respectively. These components as well as the silicone coated mylar carrier film were purchased from Richard E. Mistler, Inc.

The initial slurry mixture containing powders, solvent and dispersant was ball milled for 24 h. Then plasticizer and binder were added to the above suspension and milled for additional 5 h. Casting was performed on a laboratory tape casting unit, using a double 16-cm-wide doctor blade, at a rate of 2 cm/s. The casting gap was 400 μm. Tape drying was carried out at room temperature in the air. After drying, the tapes peeled easily off the substrate. Layers of the tape were laminated in alternating casting and cross-casting directions. The laminates (70×50×2 mm) were die pressed for 3 min at a pressure of 15 MPa at room temperature. The laminates were slowly heated to 1200°C at a heating rate of 0.3°C/min with three dwells at 185°C (3 h), 400°C (4 h), and 600°C (3 h) to burn out the organic components. Final sintering was performed at 1200°C for 4 h. The NiO was then reduced to metallic nickel at a temperature of 1000°C in a reducing atmosphere (7%H_2 in Ar).

2.3. Characterization of deposits

The phase content was determined by X-ray diffraction (XRD) with a diffractometer (Nicolet I2) using monochromatized Cu K_α radiation at a scanning speed of 0.5°/min. Thermogravimetric analysis (TG) and differential thermal analysis (DTA) were carried out in air between room temperature and 1200°C at a heating rate of 5°C/min using a thermoanalyzer (Netzsch STH-409). The microstructures of the deposited films were studied using a Philips 515 scanning electron microscope (SEM) equipped with energy dispersive spectroscopy (EDS). To prepare specimens for analysis, the green deposits were removed from Ni substrates, annealed at 400°C, pressed into discs, sintered at 1300°C and polished.

3. Experimental results

Cathodic deposits were successfully obtained from solutions of $CeCl_3$ and $GdCl_3$ in water and ethanol–water

solvents. The deposits obtained from aqueous 0.01 M $CeCl_3$ + 0.025 H_2O_2 solutions were analyzed by XRD both before and after sintering in air at different temperatures. The fresh deposits and those thermally treated at 200°C exhibited very broad peaks; however, the deposits contained a significant amount of amorphous phase (Fig. 2). On sintering the deposits at 500°C, the XRD pattern displayed the peaks of CeO_2 (JCPDS Index Card 34-394). Thermogravimetric analysis of fresh deposits obtained under these experimental conditions showed weight loss during heating (Fig. 3). Two distinct steps in the TG curve may be noted. A sharp reduction of sample weight was observed up to ~200°C, an additional step in weight loss was recorded in the range 460–520°C, then the weight fell gradually. The total weight loss in the temperature region up to 1200°C was ~50%. A broad endothermic peak around 190°C and an endotherm around 510°C are seen in the DTA curve (Fig. 3).

EDS data for deposits prepared from mixed solutions of $CeCl_3$ and $GdCl_3$ salts indicate formation of composite films, as shown in Fig. 4. X-ray studies of composite $Ce_{1-x}Gd_xO_{2-y}$ films were performed. Fig. 5 shows X-ray data for the film of composition $x = 0.2$. The XRD spectra taken from fresh deposits exhibit very broad peaks; however the deposits were essentially amorphous. The peaks become more distinct at higher temperatures, indicating formation of cubic fluorite-type structure [23–25].

In a previous investigation, no electrodeposition of PDDA was observed from pure PDDA solutions [22].

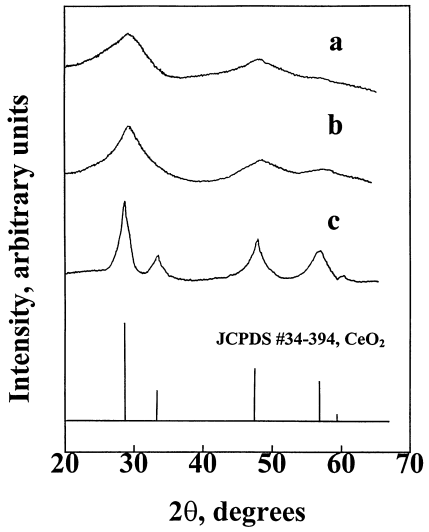

Fig. 2. X-ray diffraction patterns of the deposit obtained from aqueous 0.01 M $CeCl_3$ + 0.025 M H_2O_2 solution at current density of 5 mA/cm^2: (a) as prepared and after thermal treatment at (b) 200°C and (c) 500°C compared to JCPDS data file 34-394 for CeO_2.

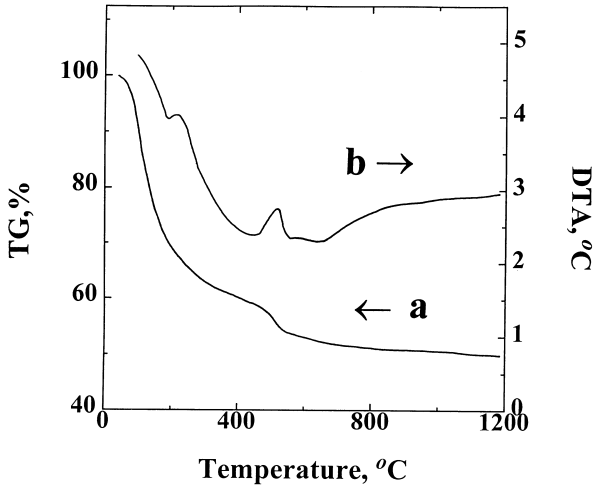

Fig. 3. (a) TG and (b) DTA data for the deposit obtained from aqueous 0.01 M $CeCl_3$ + 0.025 M H_2O_2 solution at a current density of 5 mA/cm^2.

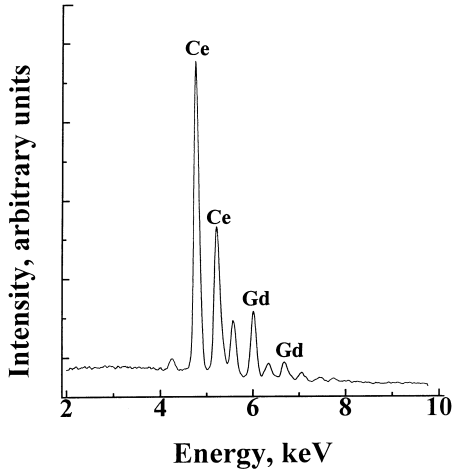

Fig. 4. EDS data for the deposit obtained from 2 mM $GdCl_3$ + 8 mM $CeCl_3$ solution in mixed ethyl alcohol–water solvent (9:1 volume ratio) saturated with air at a current density of 5 mA/cm^2.

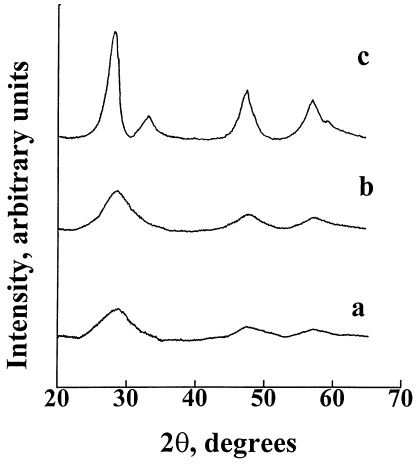

Fig. 5. X-ray diffraction patterns of $Ce_{0.8}Gd_{0.2}O_{2-y}$: (a) as prepared, after thermal treatment at (b) 200°C and (c) 500°C.

Cathodic deposits were obtained only when $GdCl_3$ was added to the solutions [22]. It was shown that gadolinium hydroxide particles precipitate at the electrode together with PDDA to form organoceramic deposits. Results of this work indicate that cathodic deposits could be obtained when $CeCl_3$ salt is added to the PDDA solutions. Fig. 6 shows dependencies of deposit weight versus salt concentration in pure $CeCl_3$ solutions and $CeCl_3$ solutions containing 1 g/l PDDA additive. For both solutions, the deposit weight increases with salt concentration, but the PDDA containing solutions had lower yields.

Fig. 7 compares TG data for deposits obtained from 0.01 M $CeCl_3$ + 1 g/l PDDA and pure PDDA dried in air. In both cases, a sharp reduction of sample weight was recorded below ~500°C, followed by a more gradual weight decrease. The total weight loss for the deposits in the temperature region up to 1200°C was ~51%.

SEM observations of ceria and doped ceria deposits obtained from aqueous solutions exhibited cracking attributed to drying shrinkage. Films obtained from mixed ethyl alcohol-water solutions and films obtained in the presence of hydrogen peroxide exhibited lower cracking. However all the deposits were inevitably cracked (Fig. 8) when their thickness was higher than 0.2–0.3 μm. In contrast, deposits obtained from mixed PDDA containing solutions exhibited enhanced resistance to cracking and were adherent to Ni substrates. Crack free organoceramic deposits were obtained from aqueous $CeCl_3$ solutions containing 0.5–1 g/l PDDA, when film thickness was in the range up to ~1 μm. Electrodeposition was also performed on Ni–YSZ substrates obtained by tape casting. The substrates were porous as shown in Fig. 9. The porosity resulted from low temperature sintering and reduction of nickel oxide

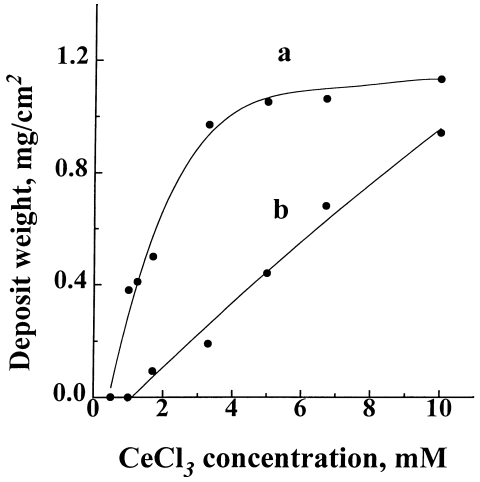

Fig. 6. Deposit weight as a function of $CeCl_3$ concentration in aqueous $CeCl_3$ solutions: (a) without additive, and (b) containing 1 g/l PDDA at constant deposition time of 20 min and current density of 5 mA/cm^2.

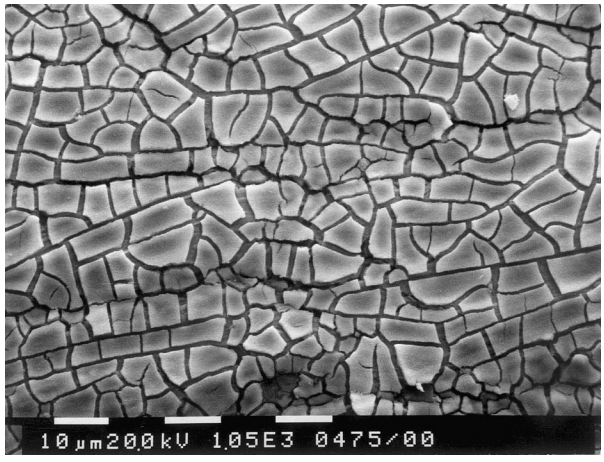

Fig. 8. SEM photograph of the electrolytic deposit obtained from 0.01 M $CeCl_3$ + 0.025 M H_2O_2 solution at a current density of 5 mA/cm^2.

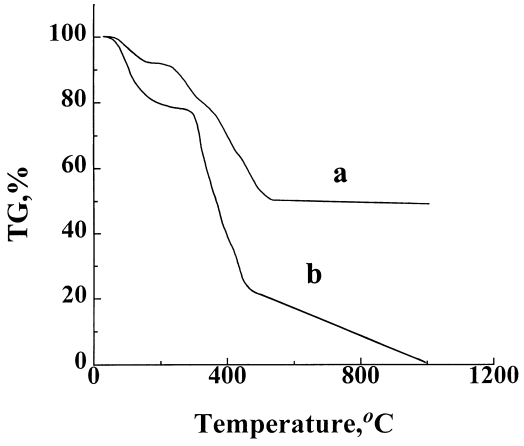

Fig. 7. TG data (a) for the deposit obtained from 0.01 M $CeCl_3$ + 1 g/l PDDA solution at a current density of 5 mA/cm^2, and (b) for starting PDDA material, dried in air.

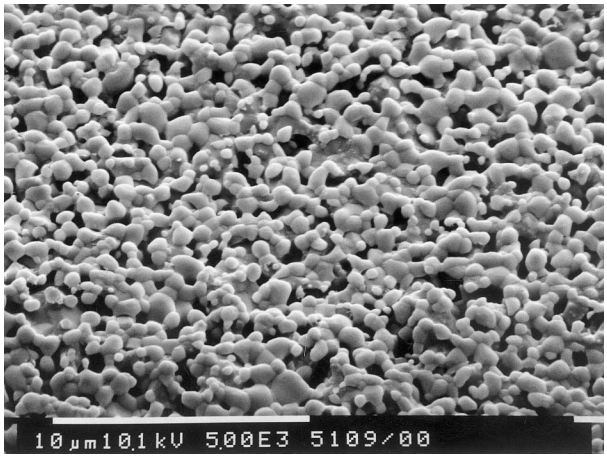

Fig. 9. SEM photograph of the Ni–YSZ cermet.

to metallic nickel. Fig. 10 shows the surface (a) and cross-section (b) of the deposit obtained from aqueous $0.01CeCl_3 + 0.7$ g/l PDDA solution. It is seen that the film is relatively continuous and pores in the substrate are mainly closed by the film. However large voids in the substrate bring about film cracking. Crack free deposits were obtained by multiple deposition when deposit thickness was about 2 microns.

4. Discussion

In the cathodic electrodeposition method, the high pH of the cathodic region brings about formation of colloidal particles, which precipitate on the electrode to form deposits. The possible electrode reactions [1,8] resulting in base generation are:

$$2H_2O + 2e^- \Longleftrightarrow H_2 + 2OH^- \quad (1)$$

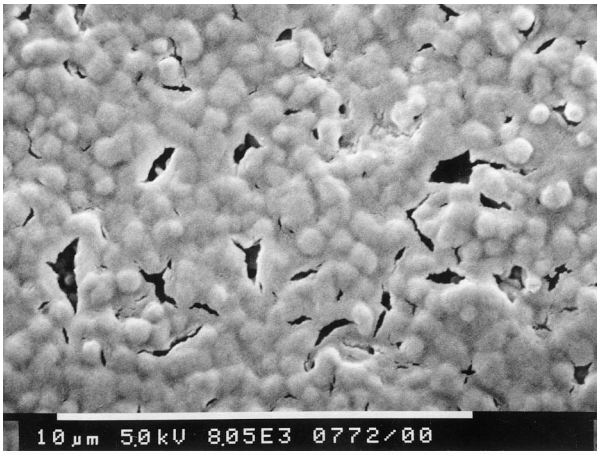

(a)

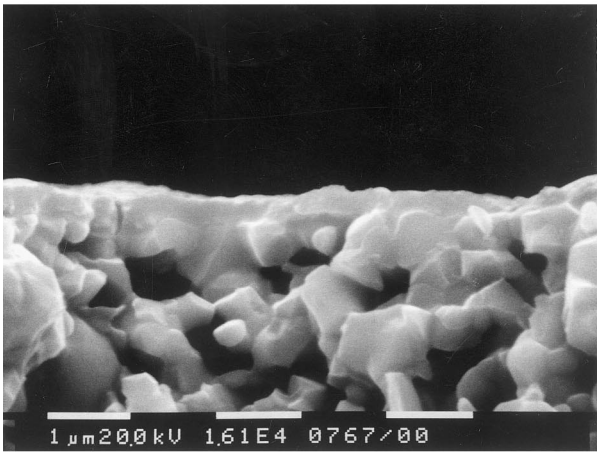

(b)

Fig. 10. SEM photographs of the deposit obtained from 0.01 M $CeCl_3 + 0.7$ g/l PDDA solution at a current density of 3 mA/cm^2 on a porous cermet substrate: (a) deposit surface and (b) cross-section.

$$O_2 + 2H_2O + 4e^- \Longleftrightarrow 4OH^- \quad (2)$$

Owing to the complex chemistry of Ce species in aqueous solutions, difficulties are encountered in identification of the scheme for reactions, which underlie the deposition process. According to Ref. [19], the valence state of cerium can be changed in alkaline solutions, containing H_2O_2 or saturated with air, and formation of $Ce(OH)^{2+}$ species can be expected. Following this scheme [19], cerium species such as $Ce(OH)^{2+}$ are hydrolyzed by electrogenerated base to form a cathodic deposit. It should be noted that wet chemical methods [1,26] resulted in precipitation of hydrated oxide $CeO_2{\cdot}nH_2O$ or $Ce(OH)_3OOH$ in solutions containing hydrogen peroxide. Therefore, it is suggested that the electrodeposition method used in this work results in the formation of $CeO_2{\cdot}nH_2O$ or $Ce(OH)_3OOH$ deposits on cathodic substrates. It is important to note that the electrodeposition method offers important advantages compared to a "cerating" process [1]. Indeed, electrodeposition allows rigid control of film thickness and deposition rate. This is in contrast to the "cerating" process [1] which resulted in formation of non-uniform deposits, containing thick, heavily cracked regions.

X-ray results indicate that cathodic deposits obtained from aqueous 0.01 M $CeCl_3$ + 0.025 M H_2O_2 solutions exhibited crystalline peaks, but the deposits were essentially amorphous. Cathodic deposition [20] of ceria from aerated solutions of $CeCl_3$ in ethanol–water solvent resulted in the formation of amorphous hydroxide deposits, which were converted to crystalline cerium oxide films after thermal treatment. In contrast, CeO_2 powders obtained by electrochemical synthesis [16] exhibited crystalline structure and no thermal treatment was used to induce crystallinity. The difference in crystallinity of fresh deposits obtained in this work, Refs. [16,20] could be attributed to different experimental conditions such as temperature, solvent, H_2O_2 additive and current density.

Thermal analysis of the deposits revealed weight loss (Fig. 3) which could be attributed to decomposition of the deposits to form CeO_2. Observed weight loss could be attributed to liberation of water and oxygen followed by the decomposition of surface carbonates at temperatures exceeding 700°C [27]. The observed endothermic peak corresponds to the weight loss. The exothermic peak is considered to be due to crystallization of CeO_2 and is in agreement with the X-ray data.

An important point to be discussed is the influence of hydrogen peroxide on electrodeposition of ceria. The role of the hydrogen peroxide is to convert Ce^{3+} to the more easily hydrolyzed Ce^{4+} species [26] and to prevent formation of nonstoichiometric cerium dioxide [28]. The experimental data presented above indicate that more adherent and uniform deposits can be obtained when hydrogen peroxide is added to aqueous $CeCl_3$ solutions.

As pointed out in [10,29] chloride ions can be partially removed from solutions through an oxidoreduction process, thus diminishing the risk of deposit contamination with chloride ions:

$$3H_2O_2 + 2HCl \Longleftrightarrow 4H_2O + O_2 + Cl_2 \quad (3)$$

The hydrogen peroxide has a number of effects on precipitates, such as conversion of the hydroxide precipitates into hydrated oxides or peroxides, and reduction of bridging and non-bridging hydroxogroups, resulting in lower aggregation [10]. It is in this regard that ceria powders were less agglomerated when hydrogen peroxide was added to cerium salt solutions [26]. In this work, the process developed for electrodeposition of ceria [20] and gadolinium oxide [22] films was extended to deposition of ceria films doped with gadolinium oxide. The crystallization behavior of electrodeposited powders was similar to that of powders prepared by other methods [23–25]. Further experiments are under way on the application of electrolytic $Ce_{1-x}Gd_xO_y$ films in fuel cells.

Note that deposit cracking associated with drying shrinkage is a common problem among wet chemical methods, once thick coatings are formed [20,30–35]. Electrolytic films studied in [34] showed less tendency to cracking when hydrogen peroxide was used as an additive. Another approach utilized in the wet chemical methods is based on the use of binders [31,33]. A method of electrochemical intercalation of binder into electrolytic deposits has recently been developed [22,36]. In this work we have extended the technique to electrolytic ceria deposits.

PDDA is a charged polymer with inherent binding properties. The polymer keeps the positive charge under basic conditions. It was expected that the cathodic electrophoretic process could be used for preparation of PDDA films. However, electrophoresis is responsible only for increasing the local concentration of charged particles in the vicinity of the cathode, and is not involved in any subsequent phenomena. Therefore, it is not surprising that no deposit formation was observed from pure PDDA solutions [22]. However, after the addition of $CeCl_3$ electrolyte to the PDDA solutions, cathodic deposits were obtained. The deposit weight increased with $CeCl_3$ concentration at a constant concentration of PDDA. In previous work [22], it was suggested that intercalation of polymer particles into the electrolytic deposit was achieved by their adsorption on the surface of colloidal particles, which are produced near the cathode and form a cathodic deposit. A model has been developed based on electrostatic attraction of oppositely charged colloidal particles of ceramic material and polymer. The amount of organic phase can be evaluated from thermogravimetric analysis [22,36]. TG data for the deposit obtained from 0.01 M $CeCl_3$ + 1 g/l PDDA showed weight loss which can be attributed to thermal decomposition of organic and inorganic phases. However, evaluation of the amount of organic phase from TG data only presents difficulties owing to complex chemistry of cerium species. Moreover, it is reasonable to assume [22] that the organoceramic deposit cannot be considered as a simple mixture of inorganic and organic phases. Experimental data from Fig. 6 indicate that deposit weights obtained from $CeCl_3$ solutions containing PDDA were lower than those without PDDA. It is suggested that PDDA particles provide shielding against deposition of cerium species. Therefore detailed investigation, currently under way, is necessary to study the composition of deposits prepared under various experimental conditions. Preliminary results of this investigation, indicate that the composition of the organoceramic deposit depends on concentration of the metal salt, PDDA concentration and current density.

The PDDA acts as a binder, promoting better adhesion of organoceramic deposits and decreasing cracking. For electrodeposition on a porous substrate from $CeCl_3$ solutions, cerium species can easily penetrate and deposit on inner surfaces of the porous network. In contrast, when PDDA is used as an additive, penetration is blocked and the deposit forms only at the top surface. It should be mentioned that thin layers of PDDA and other cationic polymers were recently used in membranes preventing ion permeation [37]. In these membranes positively charged ions receive strong repulsive force from the positively charged polymer layers. Our current efforts are concentrated on electrodeposition of organoceramic layers of graded composition containing polymer rich layers interfacing with porous substrates.

5. Conclusions

Electrodeposition of CeO_2 and $Ce_{1-x}Gd_xO_{2-y}$ was achieved via hydrolysis by electrogenerated base of $CeCl_3$ and $GdCl_3$ salts dissolved in water or mixed ethyl alcohol solvent followed by thermal decomposition of the green deposits. Results of X-ray show that fresh deposits contained amorphous phases. Deposit crystallization was observed after thermal dehydration of the amorphous precursors at 500°C. The influence of hydrogen peroxide on the deposition process has been studied. Experimental conditions were determined for electrochemical intercalation of positively charged poly(diallyldimethylammonium chloride) into the deposits. It was established that films obtained from solutions containing the cationic polymer with inherent binding properties as an additive, adhered well to the substrates and exhibited enhanced resistance to cracking. The use of the polymer restricted film formation to the top surface of a porous cermet substrate. These results may

find application in the processing of ceria and doped ceria films in fuel cells.

References

[1] A.E. Hughes, R.J. Taylor, B.R.W. Hinton, L. Wilson, XPS and SEM characterization of hydrated cerium oxide conversion coatings, Surface and Interface Analysis 23 (7/8) (1995) 540–550.

[2] S. Roure, F. Czerwinski, A. Petric, Influence of CeO_2-coating on the high-temperature oxidation of chromium, Oxidation of Metals 42 (1/2) (1994) 75–102.

[3] K. Kuribayashi, R. Uchikawa, K. Takahashi, Preparation of cerium dioxide thin films via sol–gel process and their characteristics as electrical buffer layers, Journal of the Ceramic Society of Japan 107 (3) (1999) 275–277.

[4] R. Doshi, V.L. Richards, J.D. Carter, X. Wang, M. Krumpelt, Development of solid-oxide fuel cells that operate at 500°C, Journal of the Electrochemical Society 146 (4) (1999) 1273–1278.

[5] T. Tsai, S.A. Barnett, Increased solid-oxide fuel cell power density using interfacial ceria layers, Solid State Ionics 98 (3–4) (1997) 191–196.

[6] K. Eguchi, Ceramic materials containing rare earth oxides for solid oxide fuel cell, Journal of Alloys and Compounds 250 (1997) 486–491.

[7] H. Uchida, S. Arisaka, M. Watanabe, High performance electrode for medium temperature solid oxide fuel cells $La(Sr)CoO_3$ cathode with ceria interlayer on zirconia electrolyte, Electrochemical and Solid-State Letters 2 (9) (1999) 428–430.

[8] I. Zhitomirsky, L. Gal-Or, Electrochemical coatings, in: N.B. Dahotre, T.S. Dahotre (Eds.), Intermetallic and Ceramic Coatings, Marcel Dekker Inc, New York, 1999, pp. 83–145.

[9] R. Chaim, G. Stark, L. Gal-Or, H. Bestgen, Electrochemical ZrO_2 and Al_2O_3 coatings on SiC substrates, Journal of Materials Science 29 (23) (1994) 6241–6248.

[10] I. Zhitomirsky, Electrolytic deposition of oxide films in the presence of hydrogen peroxide, Journal of the European Ceramic Society 19 (15) (1999) 2581–2587.

[11] I. Zhitomirsky, L. Gal-Or, Cathodic electrosynthesis of ceramic deposits, Journal of the European Ceramic Society 16 (8) (1996) 819–824.

[12] H. Konno, M. Tokita, R. Furuichi, Formation of perovskite structure $La_{1-x}Ca_xCrO_3$ films with electrodeposition, Journal of the Electrochemical Society 137 (1) (1990) 361–362.

[13] M. Izaki, T. Omi, Electrolyte optimization for cathodic growth of zinc oxide films, Journal of the Electrochemical Society 143 (3) (1996) L53–L55.

[14] I. Zhitomirsky, L. Gal-Or, A. Kohn, H.W. Hennicke, Electrodeposition of ceramic films from non-aqueous and mixed solutions, Journal of Materials Science 30 (20) (1995) 5307–5312.

[15] J.A. Switzer, Electrochemical synthesis of ceramic films and powders, American Ceramic Society Bulletin 66 (10) (1987) 1521–1524.

[16] Y. Zhou, R.J. Phillips, J.A. Switzer, Electrochemical synthesis and sintering of nanocrystalline cerium (IV) oxide powders, Journal of the American Ceramic Society 78 (4) (1995) 981–985.

[17] M. Balasubramanian, C.A. Melendres, A.N. Mansour, X-ray absorption spectroscopy study of the local structure of heavy metal ions incorporated into electrodeposited nickel oxide films, Journal of the Electrochemical Society 146 (2) (1999) 607–614.

[18] M. Balasubramanian, C.A. Melendres, A.N. Mansour, An X-ray absorption study of the local structure of cerium in electrochemically deposited thin films, Thin Solid Films 347 (1/2) (1999) 178–183.

[19] A.J. Aldykiewicz Jr, A.J. Davenport, H.S. Isaacs, Studies of the formation of cerium-rich protective films using X-ray absorption near-edge spectroscopy and rotating disk electrode methods, Journal of the Electrochemical Society 143 (1) (1996) 147–154.

[20] I. Zhitomirsky, A. Petric, Electrolytic and electrophoretic deposition of CeO_2 films, Materials Letters 40 (6) (1999) 263–268.

[21] F.-B. Li, R.C. Newman, G.E. Thompson, In situ atomic force microscopy studies of electrodeposition mechanism of cerium oxide films: nucleation and growth out of a gel mass precursor, Electrochimica Acta 42 (16) (1997) 2455–2464.

[22] I. Zhitomirsky, A. Petric, Electrolytic deposition of Gd_2O_3 and organoceramic composite, Materials Letters 42 (5) (2000) 273–279.

[23] J. Van Herle, T. Horita, T. Kawada, N. Sakai, H. Yokokawa, M. Dokiya, Oxalate coprecipitation of doped ceria powder for tape casting, Ceramics International 24 (3) (1998) 229–241.

[24] A. Tsoga, A. Naoumidis, W. Jungen, D. Stöver, Processing and characterization of fine crystalline ceria gadolinia-yttria stabilized zirconia powders, Journal of the European Ceramic Society 19 (6–7) (1999) 907–912.

[25] R.S. Torrens, N.M. Sammes, K. Kendall, J.C. Austin, Characterisation of dopped ceria powders prepared by wet chemical methods, in: S.C. Singhal, M. Dokiya (Eds.), Solid Oxide Fuel Cells (SOFC VI), Proceedings of the Sixth International Symposium.Vol. 99-19. The Electrochemical Society, Inc, Pennington, NJ, 1999, pp. 209–216.

[26] B. Djurićić, S. Pickering, Nanostructured cerium oxide: preparation and properties of weakly-agglomerated powders, Journal of the European Ceramic Society. 19 (11) (1999) 1925–1934.

[27] J.L.G. Fierro, S. Mendioroz, A.M. Olivan, Preparation and characterization of the catalytically active forms of rare earth oxides, Journal of Colloid and Interface Science 100 (2) (1984) 303–310.

[28] S.P. Ray, A.S. Nowick, D.E. Cox, X-ray amd neutron diffraction study of intermediate phases in nonstoichiometric cerium dioxide, Journal of Solid State Chemistry 15 (4) (1975) 344–351.

[29] I. Zhitomirsky, Electrolytic deposition of niobium oxide films, Materials Letters 35 (3/4) (1998) 188–193.

[30] I. Zhitomirsky, Electrophoretic and electrolytic deposition of ceramic coatings on carbon fibers, Journal of the European Ceramic Society 18 (7) (1998) 849–856.

[31] S. Lakhwani, M.N. Rahaman, Adsorption of polyvinylpyrrolidone (PVP) and its effect on the consolidation of suspensions of nanocrystalline CeO_2 particles, Journal of Materials Science 34 (16) (1999) 3909–3912.

[32] F. Czerwinski, J.A. Szpunar, Optimizing properties of CeO_2 sol–gel coatings for protection of metallic substrates against high temperature oxidation, Thin Solid Films 289 (1/2) (1996) 213–219.

[33] R.K. Roeder, E.B. Slamovich, Measuring the critical thickness of thin metalorganic precursor films, Journal of Materials Research 14 (6) (1999) 2364–2368.

[34] I. Zhitomirsky, L. Gal-Or, A. Kohn, M.D. Spang, Electrolytic PZT films, Journal of Materials Science 32 (3) (1997) 803–807.

[35] I. Zhitomirsky, Cathodic Electrosynthesis of titania films and powders, Nanostructured Materials 8 (4) (1997) 521–528.

[36] I. Zhitomirsky, A. Petric, Electrochemical deposition of yttrium oxide, Journal of Materials Chemistry 10 (5) (2000) 1215–1218.

[37] L. Krasemann, B. Tieke, Selective ion transport across self-assembled alternating multilayers of cationic and anionic polyelectrolytes, Langmuir 16 (2) (2000) 287–290.